0026-895X/87/030284-10$02.00/0

MOLECULAR PHARMACOLOGY, 31:284–293

Electronic Determinants of the Anti-inflammatory Action of Benzoic and Salicylic Acids

E. L. MEHLER and J. GERHARDS[1]

Department of Structural Biology, Biocenter, University of Basel, CH-4056 Basel, Switzerland

Received July 21, 1986; Accepted December 15, 1986

SUMMARY

Ab initio, quantum chemical methods have been used to study the possible modes of binding of benzoic and salicylic acids to cyclooxygenase which lead to their anti-inflammatory action. The biological data for this work were obtained from full dose response curves of the inhibitory potency of active compounds on prostaglandin production in mouse macrophages. With the help of simple regression analysis the most important reactivity indices are identified and the ionization state of the active species is discussed. From the physical significance implied by these regressions and an analysis of the electronic charge distributions of the frontier orbitals, a two-way charge transfer model is proposed. The electrostatic potentials of active and inactive congeners have been analyzed, and it is shown that an electrostatic orientation effect seems to make an important contribution to the binding of the active molecules to their receptor site. An electrostatic potential model of the binding site is proposed, and it is shown that this model is able to rationalize the source of activity or inactivity of the investigated substances.

More than a dozen possible biochemical mechanisms were suggested (1) when Vane and co-workers (2, 3) and Smith and Willis (4) demonstrated that therapeutic concentrations of indomethacin, aspirin, and salicylate inhibit the biosynthesis of prostaglandins. Since then, a wide variety of chemical classes of NSAIDs have been shown to inhibit PGS, at least in the isolated and purified enzyme (5, 6). Nevertheless, although a large body of experimental evidence has accumulated, the structural requirements of NSAID activity and even reliable quantitative structure-activity relationships are still lacking (7).

The biochemical properties of PGS have been reviewed elsewhere (5, 6), and we summarize only the most relevant aspects relating to NSAID activity. The purified enzyme is an integral membrane heme-protein located on the cytoplasmic site of the endoplasmatic reticulum with both cyclooxygenase and hydroperoxidase activity. All classical NSAIDs are inhibitors of the cyclooxygenase with little or no effect on the hydroperoxidase. In general, the inhibition can occur through different types of action (8), i.e., reversible competition (substrate-related fatty acids, most of the common NSAIDs), irreversible competition [aspirin, which acetylates a serine residue in the active site (9)], and reversible noncompetition (antioxidants such as phenols).

This work was supported by Grants 3.872-0.81 and 3.523-0.83 of the Swiss National Foundation for the Advancement of Scientific Research.

[1] Present address: Hoffmann-La Roche & Cie., Grenzacherstrasse 124, CH-4002 Basel, Switzerland.

More recently, evidence has been presented that the locus of competitive binding is not only the catalytic site, but also a supplementary site distinct from, but related to, the catalytic site (10–12). These latter studies have shown that SAA interacts more effectively at the supplementary site than at the catalytic site and prevents the inhibition of the enzyme by indomethacin and aspirin. In addition, the experimental data suggest that the supplementary site is in a highly lipophilic area of the enzyme (10).

The existence of two binding sites would help explain the difficulties encountered in rationalizing the structural requirements of NSAIDs. It would also explain why more than one receptor model seems to rationalize the binding properties of subsets of these drugs (13, 14). The most natural way to gain an understanding of structure-activity relationships at the molecular level is the explicit consideration of inhibitor-enzyme interactions on the basis of structural models. This direct path to gaining an understanding of NSAID-receptor binding is unavailable because the three-dimensional structure of PGS is unknown. In the present case, therefore, it seems that a promising alternative approach is one which concentrates on identifying those electronic interactions which may contribute to stabilizing the inhibitor-receptor complex without specifying the shape or explicit attributes of the receptor's binding sites.

In a previous paper we reported a correlation between potency and the HOMO energy of a sample of 19 substituted SAAs, BZAs and phenols (15) which implied a charge transfer

ABBREVIATIONS: NSAID, non-steroidal anti-inflammatory drug; PGS, prostaglandin synthase (cyclooxygenase); BZA, benzoic acid (and congeners); SAA, salicyclic acid (and congeners); MO, molecular orbital; HOMO, highest occupied molecular orbital; LUMO, lowest unoccupied molecular orbital; ESP, electrostatic potential.

interaction between the HOMO of the drug molecules and a low lying unoccupied orbital of the receptor. Subsequently, the sample size was augmented and the plausibility of the acidic and phenolic active compounds having a common interaction site was discussed (16).

In this paper we report the results of our search for the electronic determinants of the anti-inflammatory activity of simple congeners of SAA and BZA. The reactivity indices and electronic properties were evaluated from *ab initio* calculations in order to achieve a given level of reliability for all of the properties which might come into consideration. First, regression analysis was used to find the properties which may influence potency, and, second, these results were combined with an analysis of the frontier orbital charge distributions and electrostatic potentials to formulate an interaction model and specify the electronic features which seem to be important for the activity (or inactivity) of the substances comprising the sample. Computational constraints required that only small substituents were considered, but within this limitation they were selected to describe as wide a range in electronic properties as possible. Moreover, powerful NSAIDs can be found in both classes of these prototype compounds, i.e., diflusinal and fenamates. It is hoped, therefore, that the interaction model derived from the present studies can serve as a general model for all NSAIDs which act at the same site as the compounds considered here.

Pharmacological Data and Details of the Calculations

The biological activity used in this study is defined as the potency of a given substance to inhibit the 12-*O*-tetradecanol-phorbol-13-acetate-induced prostaglandin E_2 release from mouse macrophages and is expressed as the negative logarithm of the 50% inhibitory concentration (pIC_{50}) (17). Although the degrees of freedom in the *in vitro* assay are considerably reduced compared with *in vivo* assays, there are a number of possible side reactions which could influence drug activity beyond the desired inhibition of cyclooxygenase. These include the inhibition of the phorbol ester-stimulated, Ca-dependent phospholipase A_2 activity by Ca complexation of NSAIDs (18) and the effects of SAAs and BZAs on membrane. The latter are well known and have been measured quantitatively (19). Questionable is the influence of these effects on activity since they may perturb the lipid-protein interaction of both phospholipase A_2 and cyclooxygenase.

The pIC_{50} values for all of the active SAAs and BZAs for which MO wave functions were determined are presented in Table 1. It is noted that caution needs to be exercised in using pIC_{50} values less than 3 since the high concentrations of drug required for their determination can cause experimental difficulties (solubility, pH, cytotoxicity) (17). Indeed, we found that, for the regression analyses, the four amino- and methyl-substituted SAAs with $pIC_{50} < 3$ had to be excluded, thus leaving a sample of 18 compounds. Perusal of the pIC_{50} values given in Table 1 or the more complete set in Ref. 17 shows that the SAAs are more active than the BZAs. Actually, only a few congeners of BZA were found which showed any activity at all. In addition, the order of activity for most SAAs is 5-$R \geq$ 3-$R >$ 4-R.

Ab initio MO calculations have been carried out at the minimum basis set level of approximation. The parameters for the basis sets and programs used in these calculations have been described elsewhere (20, 21). For reasons of computational economy, standard geometries were used (22) except for the amino group, where the values were taken from the microwave determination of aniline (23), and the isopropyl group, for which a staggered conformation was used. In Ref. 20, results computed with standard (or experimental) and optimum geometries were compared and shown to be qualitatively the same.

Experimental and theoretical studies (24–27) on BZA and SAA have shown that the preferred conformation of the acidic function is always coplanar with the ring. In addition, with the two exceptions noted above, the geometries of the other substituents are chosen to preserve σ-π symmetry. Within this restriction the minimum energy conformation has been used for most cases. For the SAAs the basic conformation I

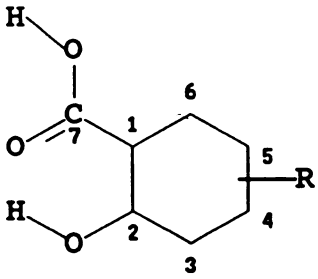

I

SCHEME 1

is taken since it is the minimum energy form for the parent compound with R = H (28). In addition, it should be noted that conformational changes in the substituent groups which result in very small changes in total energy have only small effects on the reactivity indices. For example, the maximum difference between the HOMO energies of the four conformations of *m*-OH BZA is only 1.2 kcal/mol which is to be compared with a range of 25 kcal/mol in the HOMO energies of the active BZAs and SAAs.

Using our basis sets (20), properties of aniline were calculated for various amine group bond angles. Comparison of the results indicated that they were qualitatively insensitive to limited changes in bond angle. Therefore, to further decrease computational requirements, the aniline experimental bond angle was used for all amino-substituted congeners of SAA and BZA. This choice seemed to be reasonable because *ab initio* calculations of *o*-, *m*-, and *p*-NH_2 phenols have shown that in all three cases the energies of the planar forms are at least 3 kcal/mol higher than the optimal bent forms (29). Thus, it seems unlikely that this would change in the substances considered here.

Results and Discussion

Reactivity Indices and Frontier Orbital Charge Distributions

Simple regression analysis was carried out on a large number of MO reactivity indices and any that exhibited a correlation greater than 0.6 were retained for further consideration. This low threshold was chosen because in the present complex case it cannot be expected that a single parameter can completely describe the observed activity. It was found that in several cases the 5-CH_3 and 3-NH_2 substituents were strong outliers although they never changed the physical relationship implied by the regression. Thus, in the following discussion a sample size (n) of 17 means that the 3-amino substituent was omitted and for n = 16 the 5-methyl substituent was also excluded from the calculation. In Table 1 all of the MO parameters which were found to be significant have been given.

The correlation with ϵ_{HOMO} reported previously also was found with the extended sample ($r = 0.66$, $n = 17$). In addition, a correlation with ϵ_{LUMO} was observed ($r = 0.61$, $n = 17$) which relates increasing potency with decreasing energy and implies a charge transfer interaction with the receptor acting as electron donor and the inhibitor as electron acceptor. In order to further assess the significance of these relations we investigated

TABLE 1

***In vitro* activities and reactivity indices of substituted benzoic and salicylic acids**

R	$pIC_{50} \pm cl$[a]	ϵ(HOMO)[b]	ϵ(LUMO)[b]	$D\epsilon$[b]	F_t[c]	q_π[d]	μ_x[e]	μ_y[e]
SAA								
3-NH_2	3.72 0.08	−204.74	33.63	−238.37	2.33	−0.255	1.70	−0.80
4-NH_2	2.09 0.44	−224.55	42.82	−267.37	1.52	−0.341	1.98	−0.64
5-NH_2	2.94 0.25	−202.20	31.42	−233.62	2.31	−0.253	1.70	−0.77
3-OH	4.43 0.19	−223.02	26.44	−249.47	1.63	−0.252	1.65	−0.83
4-OH	3.02 0.20	−235.88	34.66	−270.53	1.04	−0.322	1.87	−0.70
5-OH	4.61 0.36	−218.10	25.33	−243.42	1.70	−0.249	1.61	−0.83
3-CH_3	2.71 0.14	−225.86	33.37	−259.24	1.18	−0.275	1.78	−0.74
4-CH_3	2.37 0.56	−229.25	35.48	−264.73	1.05	−0.294	1.83	−0.70
5-CH_3	3.12 0.19	−223.72	33.06	−256.78	1.25	−0.274	1.76	−0.73
H	3.33 0.31	−233.21	29.87	−263.08	1.05	−0.277	1.74	−0.75
3-F	3.82 0.64	−238.17	19.99	−258.17	1.29	−0.258	1.55	−0.83
5-F	3.82 0.35	−236.00	18.66	−254.66	1.33	−0.258	1.58	−0.86
3-Cl	3.89 0.30	−234.49	20.91	−255.41	1.78	−0.267	1.61	−0.81
4-Cl	3.31 0.19	−242.47	20.72	−263.19	1.09	−0.275	1.69	−0.77
5-Cl	4.06 0.32	−232.68	20.09	−252.77	1.83	−0.266	1.61	−0.83
3-IPR′	3.92 0.24	−223.01	34.49	−257.50	1.28	−0.276	1.79	−0.73
4-IPR	3.29 0.13	−227.51	37.12	−264.63	1.07	−0.299	1.85	−0.69
5-IPR	4.12 0.54	−220.42	34.43	−254.86	1.34	−0.275	1.77	−0.71
BZA								
3,5-$(OH)_2$	3.61 0.09	−230.92	29.42	−260.35	1.14	−0.101	1.24	−0.84
3-IPR	3.01 0.07	−238.76	40.48	−279.24	0.54	−0.153	1.51	−0.69
4-IPR	2.93 0.14	−241.54	43.18	−284.72	0.49	−0.179	1.57	−0.66
4-NPR′	2.98 0.26	−243.64	43.52	−287.16	0.30	−0.176	1.56	−0.66

[a] pIC_{50} from Ref. 17. cl is the 95% confidence limits.
[b] Energies in kcal/mol. $D\epsilon = \epsilon(\text{HOMO}) - \epsilon(\text{LUMO})$.
[c] Normalized frontier orbital charge on substituents (see text).
[d] Net π-charge on fragment C_1C_7OOH.
[e] The x and y components of dipole moment contributions (in Debye) of the fragment C_1C_7OOH.
[f] IPR, isopropyl; NPR, *n*-propyl.

the correlation between pIC_{50} and $D\epsilon = \epsilon_{HOMO} - \epsilon_{LUMO}$ which is plotted in Fig. 1. The regression has the form

$$pIC_{50} = 0.0316D\epsilon + 11.85 \qquad (1a)$$
$$r = 0.80\ F = 28.1\ \text{SD} = 0.31\ n = 18$$

where r is the correlation coefficient, F the F test, and SD the standard deviation. Fig. 1 clearly illustrates the strong deviation of 5-CH_3 SAA and 3-NH_2 SAA from the regression line. The figure shows that the pIC_{50} values of these two substances are overestimated, and if they are excluded, the regression becomes

$$pIC_{50} = 0.0394D\epsilon + 13.97 \qquad (1b)$$
$$r = 0.92\ F = 76.0\ \text{SD} = 0.21\ n = 16$$

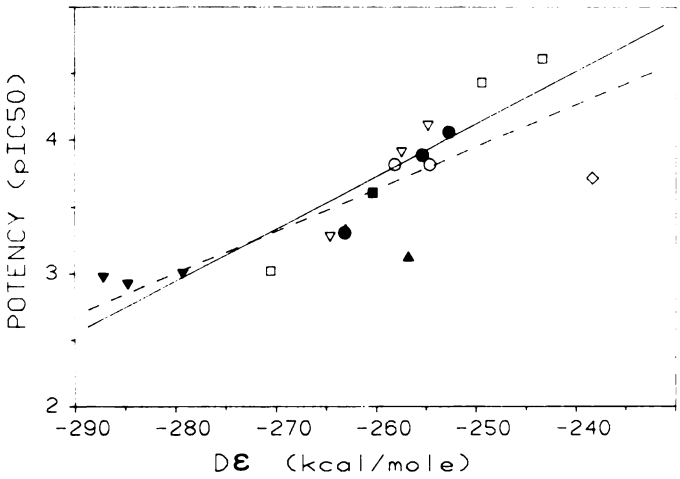

Fig. 1. Linear regression of pIC_{50} with ϵ(HOMO) − ϵ(LUMO) for substituted BZA and SAA. – – –, regression for sample of 18 compounds (Eq. 1a); —, regression for sample of 16 compounds (Eq. 1b). △, SAA; ▲, 5-methyl SAA; ▽, *i*-isopropyl SAA; ▼, *i*-isopropyl BZA; □, *i*-OH SAA; ■, 3,5-$(OH)_2$ BZA; ○, *i*-F SAA; ●, *i*-Cl SAA, ◇, 3-(NH_2) SAAs.

The correlations of pIC_{50} with $D\epsilon$ are much better than with either ϵ_{HOMO} or ϵ_{LUMO}, and it is seen that potency decreases with increasing magnitude of $D\epsilon$. Moreover, the ordering of $D\epsilon$ for each substituent group, i.e., $D\epsilon$(4-R) < $D\epsilon$(3-R) < $D\epsilon$(5-R) seems to account quite well for the observed ordering of the potencies mentioned above. The relationship given by Eq. 1 could be the result of a cooperative two-way charge transfer interaction between the drug and its receptor.

A correlation also was observed between potency and the normalized frontier orbital charge

$$F_t = (f(\text{OH}) + f(R))/|\epsilon_{HOMO}| \qquad (2)$$

where f(OH) and $f(R)$ are the frontier orbital charges on the phenolic hydroxy and non-carboxylic acid substituents, respectively. The regression has the form

$$pIC_{50} = 1.090F_t + 2.430 \qquad (3)$$
$$r = 0.87\ F = 42.0\ \text{SD} = 0.26\ n = 16$$

Roughly speaking, Eq. 3 indicates that activity increases with frontier orbital charge buildup on the OH and R groups together. Eq. 3, although complementing Eq. 1, needs to be interpreted with caution because $D\epsilon$ and F_t are highly intercorrelated ($r = 0.93$).

A complementary charge transfer effect as suggested by Eq. 1 could be achieved through local interactions of various fragments of the inhibitor with local sites of the receptor. The

charge density distributions of the frontier orbitals are given in Fig. 2 for the parent SAA and the three hydroxy-substituted congeners which are representative of the other members of the series. The HOMO is differentiated from the LUMO in that, for the former, charge is primarily localized on the ring carbons and the substituents, whereas little or no charge is found on the carboxyl group. In contrast, the LUMO's virtual charge is localized on C_1 and the acidic function with some density on other ring carbons. It is also observed that $f(OH) + f(R)$ for the 4-substituted SAA is less than that for the other two isomers. In view of Eq. 3, this is in full agreement with the experimental observation that the 4-substituted congeners are always least active.

The charge distribution exhibited by the frontier orbitals also supports a model where charge moves from a receptor site to the acidic function of the inhibitor and from the substituents and aromatic moiety of the drug molecule to another site of the receptor. In order to explore this model further, we have considered the correlation of pIC_{50} with the net charge population at different atoms and fragments. A correlation with the net π charge on the C_1COOH fragment of the SAA was observed with the regression

$$pIC_{50} = 18.04\ q_\pi(C_1COOH) + 8.647 \qquad (4)$$
$$r = 0.73\ F = 13.6\ SD = 0.33\ n = 14$$

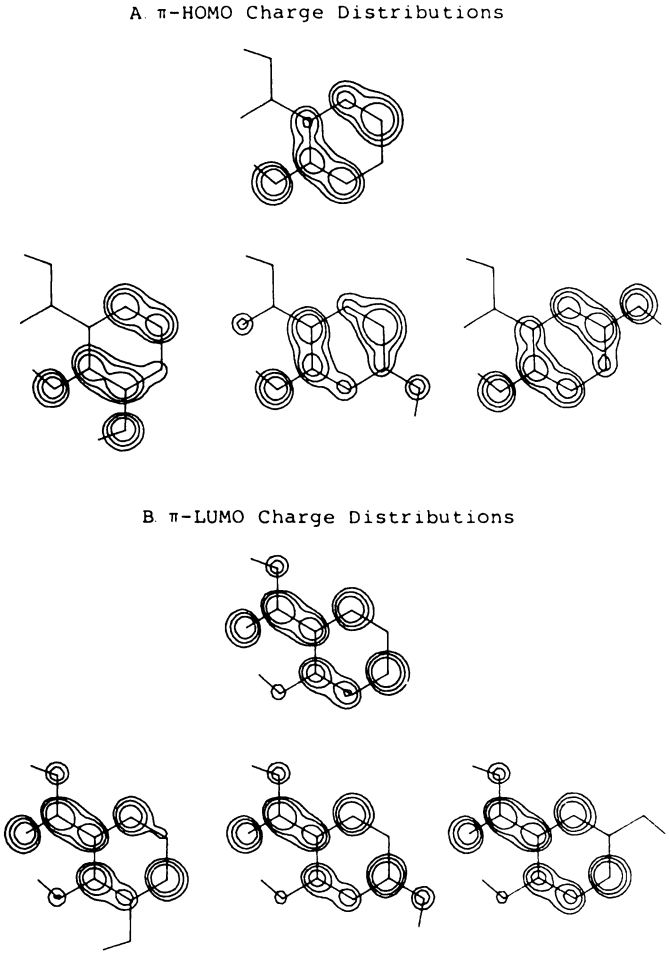

Fig. 2. π-HOMO and π-LUMO charge distributions for SAA and 3-, 4-, and 5-OH SAA. The contours are drawn 0.53 Å above the ring plane; contour values are: 0.054 $e/Å^3$, 0.027 $e/Å^3$, and 0.0135 $e/Å^3$.

which is plotted in Fig. 3. The regression line shows that activity increases with decreasing electronic charge in the C_1COOH moiety. The four BZAs form a separate group which, however, shows the same trend. Similar correlations are found with the x and y components of the dipole moment in this fragment, where activity increases with decreasing μ_x or μ_y. The result on the fragment's dipole moment vector is a rotation which is effectively equivalent to the movement of negative charge out of the fragment with increasing activity, implying the same relationship as with q_π.

The shift of charge indicated by these correlations lends further support to the interaction model proposed above. Thus, the shifting of π-charge out of the carboxyl fragment to other regions of the inhibitor could enhance the propensity for a charge transfer interaction between the drug molecule's HOMO and low lying unoccupied orbitals of the receptor, and at the same time this charge depletion makes the C_1COOH moiety more receptive to a charge transfer interaction between high lying occupied orbitals of the receptor and the inhibitor's LUMO.

Active Species

Since the pK values of the acids studied in this work lie between 3 and 4, the dissociated species predominate in the plasma and at the pH of inflamed tissue. The ionization state of the active species, however, is unknown, and it is of interest to examine the possible correlations of potency with reactivity parameters of the anions. For the corresponding anions of the SAA used in Eq. 1a, the correlations of pIC_{50} with the HOMO and LUMO energies were less than 0.3 (exclusion of 3-NH_2 SAA and 5-CH_3 SAA did not increase r). We therefore assume that either the neutral species or the anion bound to a positive interaction site is the active species. The former assumption is favored in some respect from the observations in a recent study of aspirin- and arachidonate-induced inactivation of platelet cyclooxygenase (30). In these studies methylsalicylates were found to be more active than SAA in inhibiting platelet aggregation. This result implies that the anionic carboxylate moiety of SAA does not participate in the interaction since, otherwise, esterification would reduce activity.

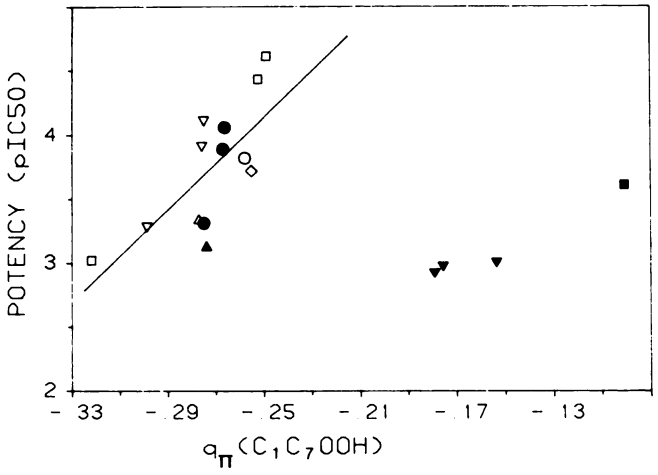

Fig. 3. Linear regression of pIC_{50} with $q_\pi(C_1C_7OOH)$, Eq. 4. For symbols see legend to Fig. 1.

Electrostatic Potentials

The effectiveness of the reactivity index, $D\epsilon$, to describe the potency may be seen from Table 2 where the calculated pIC_{50} values using Eq. 1b are given for the active substances and a number of inactive BZA congeners. Considering the fact that Eq. 1b has only one dependent variable, the measured pIC_{50} values are reasonably well reproduced. Nevertheless, there are five inactive BZAs which are predicted to be active, i.e., those congeners with $pIC_{50} > 3.0$.

The fact that $D\epsilon$ cannot completely separate active from inactive substances suggests that additional factors, not described by this parameter, are operative in the process leading to complex formation. Since the ESP is very effective in providing additional insight into the electronic effects which contribute to activity (31), we have calculated ESP maps for most of the active compounds and a large number of inactive congeners of BZA (see Table 2).

The ESP maps for the prototype molecules SAA and BZA are given in Fig. 4. The most significant difference is the shift of the deep potential minimum from the region near the carboxylate oxygen to the region below the phenolic oxygen. Since all these molecules also have a minimum over the aromatic ring, the difference between the vectors connecting this latter minimum to the minimum near the one or the other oxygen in the two molecules is a rotation of about 45–60°. A similar phenomenon between the most and least active substances was noted by Weinstein *et al.* (32) in their studies of the interactions of hydroxytryptamines with the LSD-serotonin receptor. The above vectors were termed "orientation" vectors, i.e., the lines connecting the potential minima through areas of steepest change (33). The appearance of orientation vectors as determinants of reactivity implies a direct contribution to the free energy of interaction from the alignment of the pharmacophore with the reaction site. Insofar as the interacting pharmacophore has to assume an unfavorable conformation to achieve optimal (stabilizing) alignment of the electrostatic force field or an optimal alignment is inaccessible, the interaction free energy and, hence, the binding will be weakened. In the substances studied here, the orientation vector found for SAA (the solid vector in Fig. 4b) was practically essential for activity. If a comparably deep minimum (the vector in Fig. 4a or dashed vector in Fig. 4b) was also present at the carboxylate oxygen, the potency was usually weakened.

Another difference in the ESP of BZA and SAA is the increase of the positive potential around the carboxyl group of the latter. Although this difference is smaller than the change leading to the rotation of the orientation vectors, it does help support that part of the charge transfer model which suggests that charge moves from the receptor to the acidic region of the drug molecule. Finally, excess positive potential in the region below C_3 of I (Fig. 4a) may weakly inhibit potency, although it does not appear to be enhanced by negative potential.

The ESP maps of several hydroxy-substituted congeners of SAA and BZA are compared in Fig. 5. It is clear that the main

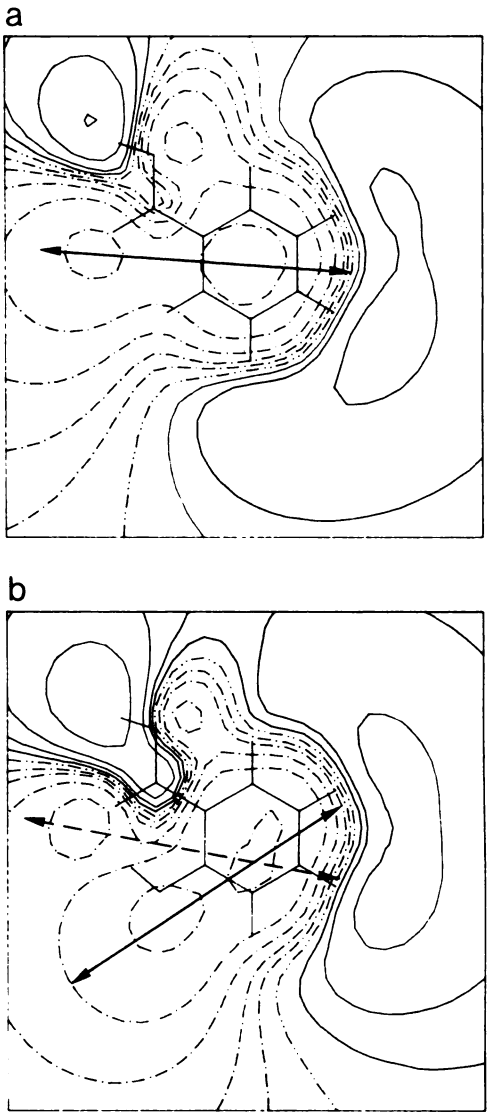

Fig. 4. ESP map 2 Å above ring plane of BZA (a) and SAA (b). Contour values (in kcal/mol) are 0, 1, 2, 4, 8, and 16. —, positive potential; –·–, negative potential; –··–, zero potential. *Arrows* indicate orientation vectors. In b (and other SAA diagrams) the solid vector is "activating" and the dashed vector is "inactivating."

TABLE 2

Calculated pIC_{50} from Eq. 1b for active and inactive acids

R	Active		Inactive BZA	
	pIC_{50}	Error[a]	$D\epsilon$[b]	pIC_{50}
	SAA			
3-OH	4.14	0.28	−266.8	3.5
4-OH	3.31	−0.30	−279.4	3.0
5-OH	4.38	0.23	−266.6	3.5
5-CH_3	3.85	0.73	−281.6	2.9
H	3.61	−0.28	−289.1	2.6
3-F	3.80	0.01	−280.7	2.9
5-F	3.94	−0.12	−279.7	2.9
3-Cl	3.91	−0.09	−274.6	3.1
4-Cl	3.60	−0.29	−277.3	3.0
5-Cl	4.02	0.04	−273.8	3.2
3-IPR[c]	3.83	0.09		
4-IPR	3.54	−0.26		
5-IPR	3.93	0.19		
	BZA			
3,5-$(OH)_2$	3.71	−0.11	−266.4[d]	3.5[c]
4-NPR[c]	2.66	0.32		
3-IPR	2.97	0.04		
4-IPR	2.76	0.22		

[a] Error = pIC_{50} (measured) − pIC_{50} (calculated); for measured values see Table 1.
[b] See Table 1, Footnote *b*.
[c] See Table 1, footnote *f*.
[d] 3,4-$(OH)_2$ BZA.

features of the parent compounds, including the alignment of the orientation vectors, are preserved in these substances. It should also be noted that conformational changes of the substituent groups will have only small effects on the orientation vectors. For example, if in Fig. 5b the OH proton is rotated 180° about the C_4—O bond, the positive and negative potential regions around this group will change places, but the orientation vectors drawn in Fig. 5b will remain essentially unchanged. In comparison to the hydroxy substituents, the activating potential minimum of the halogen-substituted SAA are somewhat shallower than the former, whereas the inactivating potential minimum is a little deeper, which is in agreement with their

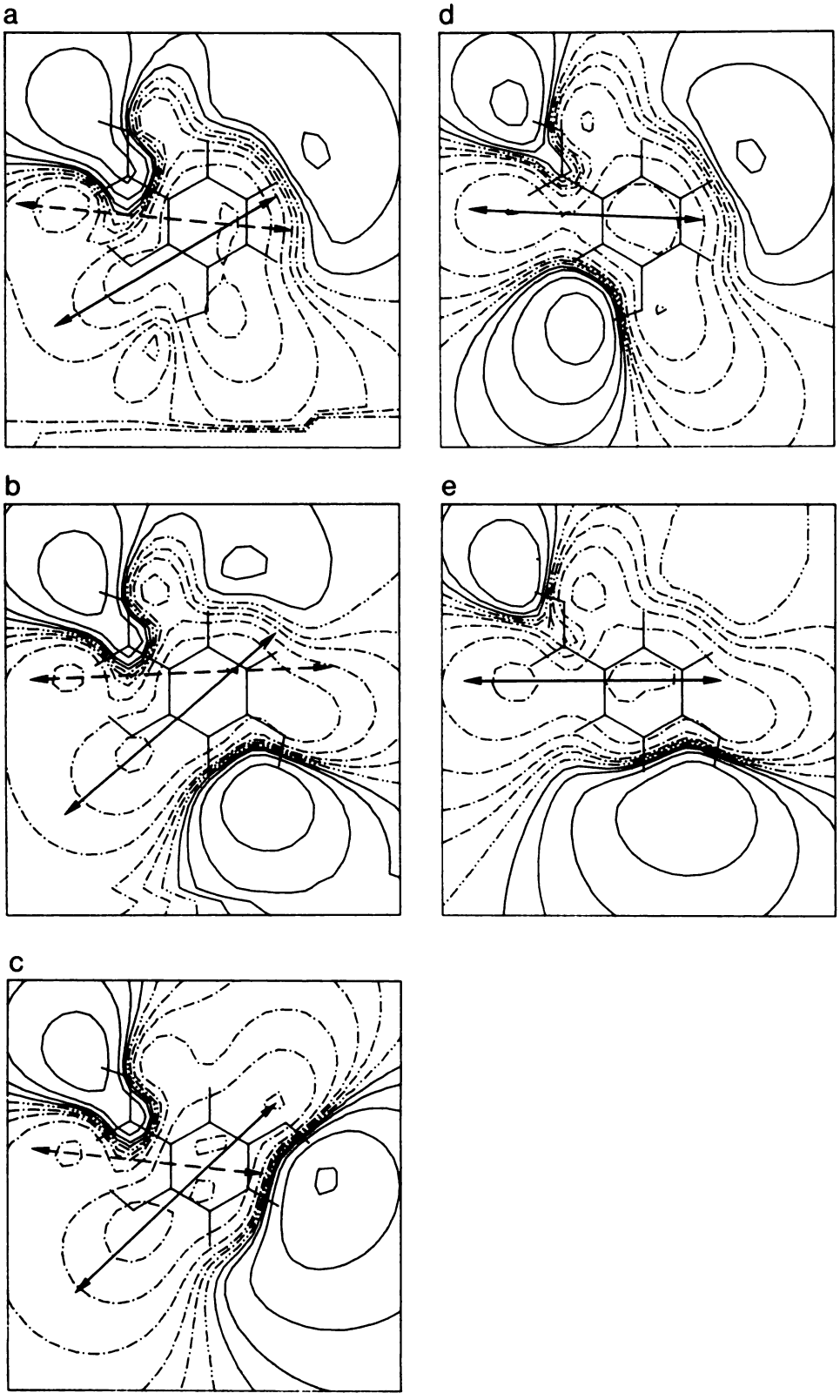

Fig. 5. ESP map of 3-OH SAA (a), 4-OH SAA (b), 5-OH SAA, (c), 3-OH BZA (d), and 4-OH BZA (e). For contour values see legend to Fig. 4. The highest contour value in c and d is 15 kcal/mol.

observed lower activity. Nevertheless, it is not clear why 4-F SAA was not observed to be active. All of our results would suggest a pIC_{50} value of about 3.2.

The fact that orientation effects seem to be important for the formation of a NSAID-receptor complex allows a model of the receptor site to be formulated based on the assumption that a complementary ESP leads to optimal binding. A schematic presentation of the hypothetical receptor site model is given in Fig. 6 with SAA shown in its presumed orientation. The two main regions of interaction are the negative potential complementary to the positive region around the carboxyl group, as shown in Fig. 4b, and a region of positive potential with its orientation vector connecting the maxima. Fig. 6 also shows the location of the most important high lying occupied and low lying unoccupied orbitals in the receptor. These locations are assumed on the basis of the charge distributions given in Fig. 2 and the relationship given by Eq. 3.

The positioning of SAA in Fig. 6 assumes that its orientation vector is parallel to that of the receptor site model. Further stabilizing effects arise through the interaction of the positive potential around the carboxyl group with the negative potential region in the binding site. Moreover, the HOMO and LUMO charge distributions given in Fig. 2 show that the optimal orientation assumed on the basis of the ESPs also leads to good overlap between these orbitals and the complementary orbitals of the binding site model, thereby enhancing charge transfer interactions in SAA. From Fig. 2 and Fig. 5, a–c, it is clear that the same stabilizing interactions apply to the hydroxy-substituted SAA. Furthermore, the extra charge density on the substituent yields an additional possibility for charge transfer stabilization for the 3- and 5-substituted isomers, but not for the 4-substituents, which also helps rationalize the observed weaker potency of the 4-substituted SAA.

Now consider complex formation with BZA: in order to achieve optimal orientation, the molecule has to be rotated so that its orientation vector is parallel with the receptor's orientation vector. However, in this orientation the negative potential associated with the lone pair of the oxygen in the carboxyl OH group (negative region between C_1 and C_6 in Fig. 4a) overlaps the negative potential of the receptor model and leads to repulsive interactions. In addition, the virtual charge distribution around C_1—C_7 shown in Fig. 2b (the LUMO charge distribution of BZA is nearly the same as SAA) is no longer properly aligned to affect the charge transfer interaction. For the substituted BZA shown in Fig. 5, d and e, the same unfavorable interactions arise. Moreover, the HOMO charge density on the substituents cannot properly align with the virtual charge of the unoccupied receptor orbitals.

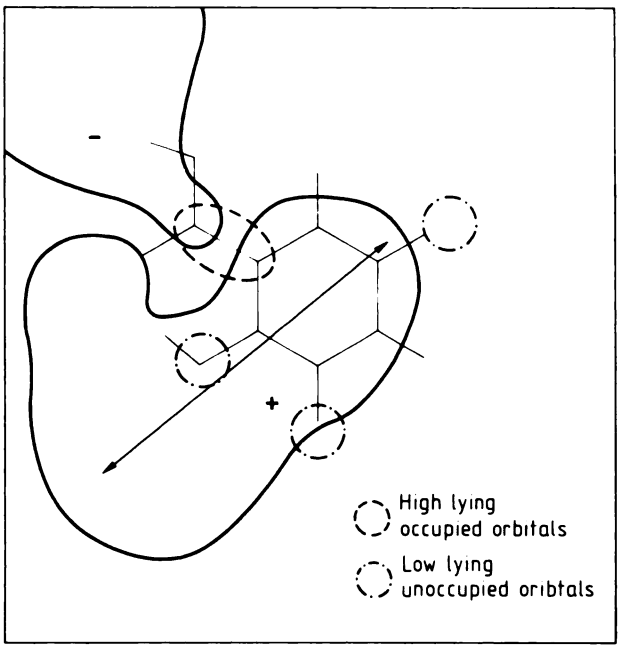

Fig. 6. Schematic presentation of proposed binding site ESP and orientation vector with locations of occupied and unoccupied orbitals which interact with inhibitor frontier orbitals. SAA is drawn in for reference.

These considerations show that the hypothetical binding site model proposed here gives quite a reasonable rationalization for the observed activity of the SAA congeners and inactivity of the BZA congeners. Some additional insight into the origin of the differences in potency of the SAA is also provided. The above arguments suggest that complex formation consists of a primary step under ESP control, and a second step controlled by charge transfer interactions. The primary step has to lead to stabilization and proper alignment of the HOMO and LUMO charge densities in the binding site for the complex to form at all and, subsequently, increasing ease of charge transfer then leads to increasing potency. This mechanistic viewpoint helps to explain the fact that some substances are inactive or much less active than predicted by their HOMO and LUMO energies and also shows the close relationship of the ESPs and frontier orbital energies in controlling potency.

The observed difference in activity between 3,4-$(OH)_2$ BZA and 3,5-$(OH)_2$ BZA is not correctly predicted from Eq. 1. It is of interest to see whether the binding site model provides a rationalization. Fig. 7a gives the ESP map of 3,5-$(OH)_2$ BZA, but no activating orientation vector appears to be present. If the map is rotated 180° about the C_1—C_7 bond, Fig. 7b results, and it is seen that an orientation vector close to the SAA vector can be drawn. The alignment of 3,5-$(OH)_2$ BZA given in Fig. 7b differs from that in Fig. 7a only in the positions of the protons. It does not disturb the two-way charge transfer interaction model proposed above (Fig. 2), but would seem to make the possibility of the carboxyl group's involvement in hydrogen bonding less likely. Moreover, superposition on the binding site model shows that the frontier orbitals still overlap the complementary orbitals of the binding site. The overlap is not as good as in 3- or 5-(OH) SAA which is in agreement with its lower activity. 3,4-$(OH)_2$ BZA was found to be inactive although it was predicted as active (Table 2). Fig. 7, c and d, gives the ESP map in the standard and rotated orientations, respectively. In neither case is an activating orientation vector found.

The case of *m*-OH BZA (Fig. 5d) is also of interest. Four conformations can be constructed, and, for two of these, activating orientation vectors can be drawn. However, assuming a Boltzman distribution at a temperature of 25°, the mole fraction of the relevant isomers is only 0.19, suggesting that their concentrations may be too small for observing activity.

It has already been observed that the measured pIC_{50} values of the amino-substituted SAA are considerably less than what would be expected from their $D\epsilon$ values. From the binding site model this can be rationalized if the ESPs of these substituents do not allow their proper alignment for complex formation. The maps of 3-NH_2 SAA, 2 Å above and below the plane are plotted in Fig. 8. Due to the pyramidal geometry of the amino

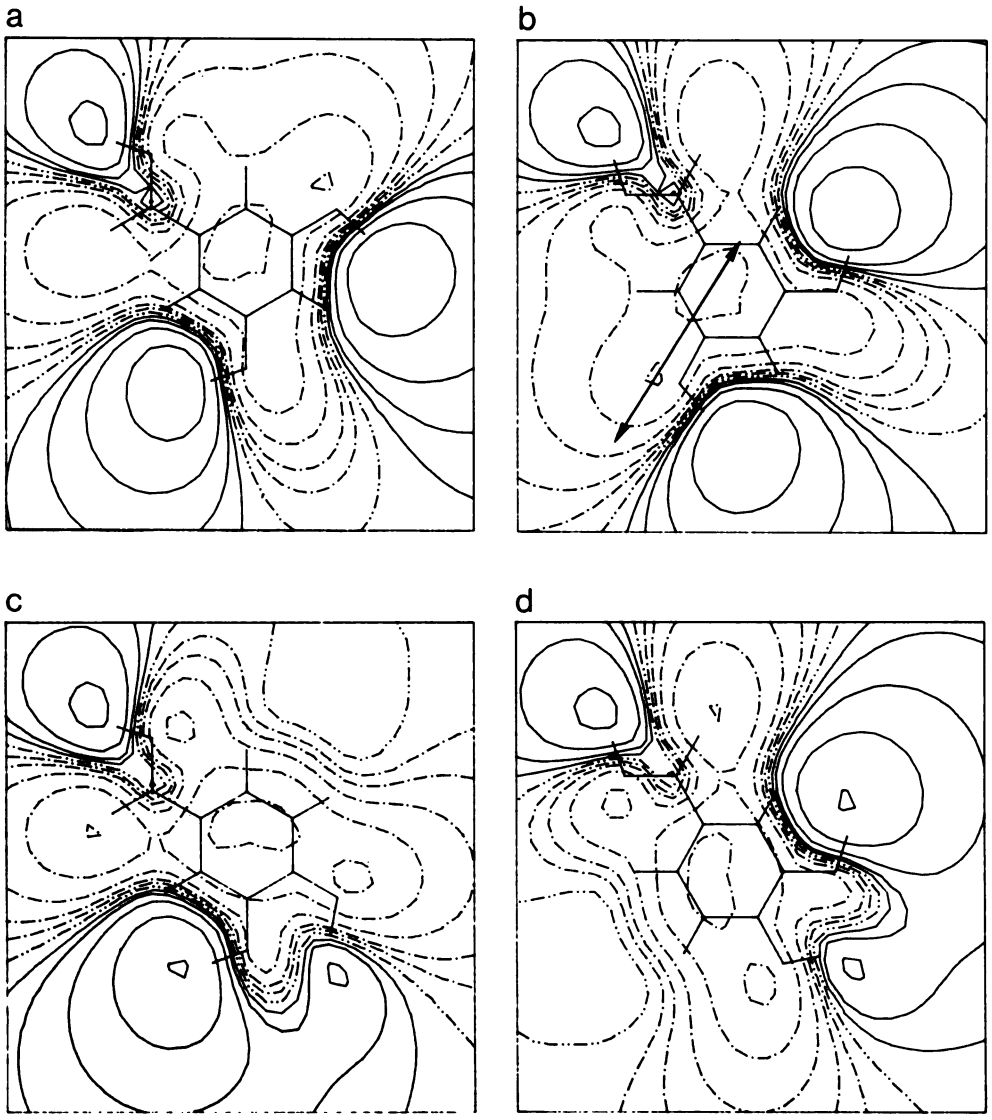

Fig. 7. ESP map of 3,5-$(OH)_2$ BZA (a), 3,5-$(OH)_2$ BZA rotated 180° about the C_1-C_7 bond (b), 3,4-$(OH)_2$ BZA (c), and 3,4-$(OH)_2$ BZA rotated 180° about the C_1-C_7 bond (d). Contour values are as in Fig. 4 except that the highest contour is 15 kcal/mol.

group, the planar symmetry of the other molecules has been lost. In reactions, the symmetries of the reacting species make an entropic contribution to the free energy, depending on the symmetry numbers of the reactants and products (34). In the present case this entropic contribution is $R\ln 2$ except for the amino-substituted SAA, where this contribution is zero. Naturally, the ESPs above and below the molecular plane may both show features indicating activity and contribute to the free energy. Fig. 8a shows a clear activating orientation vector below the molecular plane, although the minimum is fairly weak. There also is a positive potential in the region below C_3 due to the hydrogens which protrude below the plane. The map above the plane does not indicate a clear maximum near the phenolic oxygen but does show one near the carboxylate oxygen. The ESPs for the other two amino congeners show similar features which may lead to loss or decrease of activity including, in some cases, fairly strong inactivating orientation vectors. Thus, in the amino-substituted SAA the high activity implied from the $D\epsilon$ values is offset by deactivating features in their ESPs.

Conclusions

A two-step model has been proposed for the binding of substituted BZA and SAA to cyclooxygenase. The first step is an alignment of the inhibitor molecule in the binding site which is controlled by stabilizing interactions originating in the ESP of the inhibitor and the receptor's binding site. In a favorable orientation the drug molecule's frontier orbitals overlap with complementary orbitals in the binding site which then leads to the second step, consisting of a two-way charge transfer interaction. The latter step was suggested from the correlation of potency with MO reactivity indices and an analysis of the frontier orbital charge distributions, whereas the former was proposed on the basis of ESP-controlled orientation effects which strongly differentiate active from inactive substances.

The results obtained from the reactivity indices and the ESPs are complementary since the former seem able to describe quantitatively the potency of the active substances quite well, whereas the latter provide a qualitative separation between active and inactive compounds and allow a partial rationalization of some trends and deviations observed in the measured potencies. Finally, regressions on the HOMO and LUMO energies of the anions suggested that the active species consist of either the ion bound to a positive reaction center or the neutral species. Experimental evidence supports the latter assumption (30) to some extent.

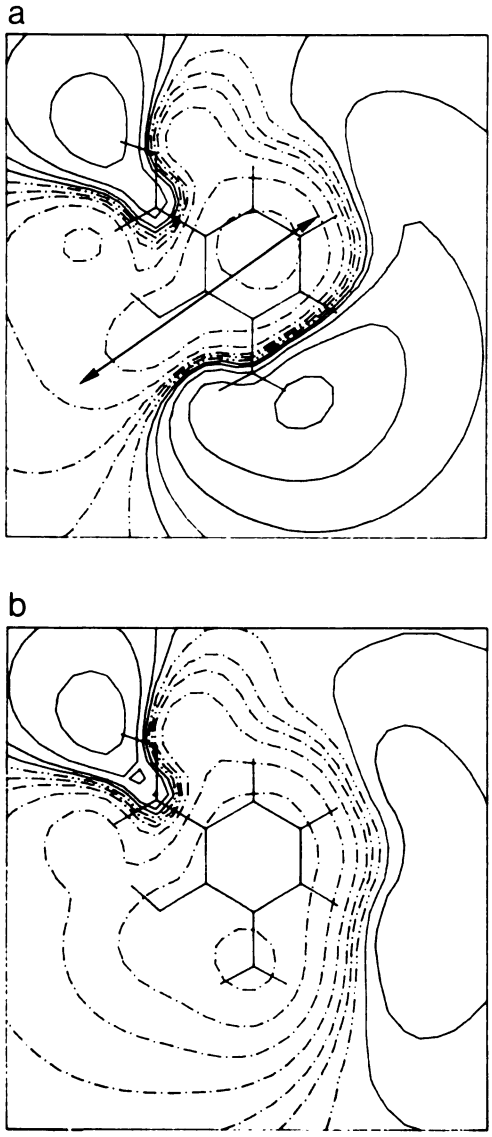

Fig. 8. ESP map of 3-NH_2 SAA, 2 Å below ring plane (a) and 2 Å above ring plane (b). Contours are as in Fig. 4; b has an additional contour at −32 kcal/mol.

Due to the existence of at least two binding sites in PGS, it is not easy to assess the generality of the present model. As was argued in comparing the acidic and phenolic NSAIDs in an earlier paper (16), it is possible that they may have one common interaction site and a second site which differs for the two classes, which would make generalizations difficult. Clearly, it would be helpful if active substances could be more consistently preclassified, either experimentally or theoretically, according to their binding site preference with PGS.

Acknowledgments

We would like to thank the University of Basel Computing Center for generous grants of computing time to carry out this research.

References

1. Brune, K., M. Glatt, and P. Graf. Mechanisms of action of anti-inflammatory drugs. *Gen. Pharmacol.* **7**:27–33 (1976).
2. Vane, J. R. Inhibition of prostaglandin synthesis as a mechanism of action for aspirin-like drugs. *Nature New Biol.* **231**:232–235 (1971).
3. Ferreira, S. H., S. Moncada, and J. R. Vane. Indomethacin and aspirin abolish prostaglandin release from the spleen. *Nature New Biol.* **231**:237–239 (1971).
4. Smith, J. B., and A. L. Willis. Aspirin selectively inhibits prostaglandin release production in human platelets. *Nature New Biol.* **231**:235–237 (1971).
5. Samuelsson, B., M. Goldyne, E. Granström, M. Hamberg, S. Hammarström, and C. Malmsten. Prostaglandins and thromboxanes. *Annu. Rev. Biochem.* **47**:997–1029 (1978).
6. Pace-Asciak, C. R., and W. L. Smith. Enzymes in the biosynthesis and catabolism of the eicosanoids: prostaglandins, thromboxanes, leukotrienes and hydroxy fatty acids. *Enzymes* **16**:543–603 (1983).
7. Gund, P., and N. P. Jensen. Nonsteroidal antiinflammatory and antiarthritic drugs, in *Quantitative Structure-Activity Relationships of Drugs* (J. G. Topliss, ed.). Academic Press, New York, 285–327, (1983).
8. Lands, W. E. M. Actions of antiinflammatory drugs. *Trends Pharmacol. Sci.* **2**:78–80 (1981).
9. Roth, G. J., E. T. Machuga, and J. Ozols. Isolation and covalent structure of the aspirin-modified, active-site region of prostaglandin synthase. *Biochemistry* **22**:4672–4675 (1983).
10. Humes, J. L., C. A. Winter, S. J. Sadowski, and F. A. Kuehl, Jr. Multiple sites on prostaglandin cyclooxygenase are determinants in the action of nonsteroidal antiinflammatory agents. *Proc. Natl. Acad. Sci. USA* **78**:2053–2056 (1981).
11. Cerletti, C., M. Livio, and G. DeGaetano. Non-steroidal anti-inflammatory drugs react with two sites on platelet cyclooxygenase. *Biochim. Biophys. Acta* **714**:122–128 (1981).
12. Cerletti, C., M. Livio, M. G. Doni, and G. DeGaetano. Salycilate fails to prevent the inhibitory effect of 5,8,11,14-eicosatetraynoic acid on human platelet cyclooxygenase and lipoxygenase activities. *Biochim. Biophys. Acta* **759**:125–127 (1983).
13. Gund, P., and T. Y. Shen. A model for the prostaglandin synthetase cyclooxygenase site and its inhibition by antiinflammatory arylacetic acids. *J. Med. Chem.* **20**:1146–1152 (1977).
14. Appleton, R. A., and K. Brown. Conformational requirements at the prostaglandin cyclooxygenase receptor site. *Prostaglandins* **18**:29–32 (1979).
15. Mehler, E. L., J. Habicht, and K. Brune. Quantum chemical analysis of structure-activity relationships in nonsteroidal anti-inflammatory drugs. *Mol. Pharmacol.* **22**:525–528 (1982).
16. Gerhards, J., and E. L. Mehler. Towards a quantum chemically derived interaction model for nonsteroidal antiinflammatory drugs: quantitative structure-activity relationships for substituted benzoic and salicylic acids and phenols, in *QSAR and Strategies in the Design of Bioactive Compounds* (J. K. Seydel, ed.). Verlag Chemie, Weinheim, 153–161 (1985).
17. Habicht, J., and K. Brune. Inhibition of prostaglandin E_2 release by salicylates, benzoates and phenols: a quantitative structure-activity study. *J. Pharm. Pharmacol.* **35**:718–723 (1983).
18. Fransen, R. X., D. Eisen, R. Jesse, and C. Lanni. Inhibition of highly purified mammalian phospholipase A_2 by nonsteroidal antiinflammatory agents. *Biochem. J.* **186**:633–636 (1980).
19. Levitan, J., and J. L. Baker. Salicylate: a structure-activity study of its effects on membrane permeability. *Science (Wash. D. C.)* **176**:1423–1425 (1972).
20. Graf, P., and E. L. Mehler. Evaluation of small Gaussian basis sets for *ab initio* calculations on biologically active molecules. *Int. J. Quantum Chem. Symp.* **8**:49–61 (1981).
21. Mehler, E. L. Self-consistent, nonorthogonal group function approximation for polyatomic systems. II. Analysis of noncovalent interactions. *J. Chem. Phys.* **74**:6298–6306 (1981).
22. Pople, J. A., and M. Gordon. Molecular orbital theory of the electronic structure of organic compounds. I. Substituent effects and dipole moments. *J. Am. Chem. Soc.* **89**:4253–4261 (1967).
23. Lister, D. G., K. K. Tyler, J. M. Hog, and N. W. Larsen. The microwave spectrum and dipole moment of aniline. *J. Mol. Struct.* **23**:253–264 (1974).
24. Böhm, S., and J. Kuthan. Optimization of molecular geometry of parasubstituted benzoic acids and their anions by means of gradient CNDO/2 method. *Collect. Czech. Chem. Commun.* **47**:3393–3409 (1982).
25. Sundaralingam, M., and L. H. Jensen. Refinement of the structure of salicylic acid. *Acta Crystallogr.* **18**:1053–1058 (1965).
26. Catalan, J., and J. J. Fernandez-Alonso. Study of the conformers of ortho- and diortho-hydroxybenzoic acid. *Chem. Phys. Lett.* **18**:37–40 (1973).
27. Bruno, G., nd L. Randaccio. A refinement of the benzoic acid structure at room temperature. *Acta Crystallogr. Sect. B Struct. Crystallogr. Cryst. Chem.* **36**:1711–1712 (1980).
28. Dietrich, S. W., E. C. Jorgensen, P. A. Kollman, and S. Rothenberg. A theoretical study of intramolecular hydrogen bonding in ortho-substituted phenols and thiophenols. *J. Am. Chem. Soc.* **98**:8310–8324 (1976).
29. Pross, A., and L. Radom. A theoretical approach to substituent interactions in substituted benzenes. *Prog. Phys. Org. Chem.* **13**:1–61 (1981).
30. Rotilio, D., D. Joseph, M. Hatmi, and B. B. Vargaftig. Structural requirements for preventing the aspirin- and the arachidonate-induced inactivation of platelet cyclooxygenase: additional evidence for distinct enzymatic sites. *Eur. J. Pharmacol.* **97**:197–208 (1984).
31. Politzer, P., and D. G. Truhlar. *Chemical Applications of Atomic and Molecular Electrostatic Potentials.* Plenum Press, New York (1980).
32. Weinstein, H., D. Chou, S. Kang, C. L. Johnson, and J. P. Green. Reactivity characteristics of large molecules and their biological activity: indole-alkylamines on the LSD-serotonin receptor. *Int. J. Quantum Chem.* **QBS3**:134–150 (1976).

33. Weinstein, H., J. P. Green, R. Osman, and W. D. Edwards. Recognition and activation mechanisms on the LSD/serotonin receptor: the molecular basis of structure-activity relationships, in QuaSAR *Research Monographs* (G. Barnett, M. Tisie, and R. Willette, eds.), Vol. 22. National Institute on Drug Abuse, Bethesda, MD, 333–357 (1978).
34. Kirkwood, J. G., and F. H. Westheimer. The electrostatic influence of substituents on the dissociation constants of organic acids. I. *J. Chem. Phys.* **6**:506–512 (1938).

Send reprint requests to: Dr. E. L. Mehler, Department of Structural Biology, Biocenter, University of Basel, CH-4056 Basel, Switzerland.